Optica Applicata, Vol. XIX, No. 3, 1989

Production of gratings for the moire interferometry method using two point light sources

S. KOZAK

Warsaw University of Technology, Institute of Design of Precise and Optical Instruments, ul. Chodkiewicza 8, 02–525 Warszawa, Poland.

The paper presents the properties of the diffraction gratings recorded for the moire interferometry method of analysis of strains by using two point sources of light. The investigation shows that the grating lines of hyperbolic-shape introduce the aberration of coma to the inteferogram obtained in the moire interferometry setup, while the asymmetry in the recording setup causes additionally astigmatism-type aberration. Small defocuses of the collimators used for recording the gratings with plane wave fronts introduce the aberrations of many types. Typical interferograms can help us to remove the inaccuracies from the recording setup.

1. Introduction

The moire interferometry method has become a well-established technique for the whole-field high sensitivity determination of in-plane displacements of deformed objects [1], [2].

Two plane waves illuminate symmetrically a reflective-type diffraction grating fixed to the specimen under study. Due to the matching of incidence angles of impinging beams with respect to the first-order diffraction angle of the grating, the $+1$ diffraction order of one illuminating beam and the -1 order of the other beam coincide in space. They propagate along the normal of specimen grating. Because of the specimen loading, the grating lines are no longer straight and the wavefronts of interfering beams are no longer plane. Their deformations due to in-plane displacements are in both diffracted beams equal but reversed longitudinally. In both beams, however, the wavefront deformations caused by out-of-plane displacements are of the same value and sign. In consequence, the amplitudes of wavefronts mutually substract during the interference, and the moire interferometry method is said to be insensitive to out-of-plane displacements. The observed fringes give information about the in-plane displacements with a basic sensitivity of half a period of the specimen grating. Special modifications of the method based on the production of conjugate interferograms permit us to obtain out-of-plane displacements [3], [4]. Gratings used in these studies are of high frequency (600–1200 l/mm) and their requirements with respect to the line straightness are also high. There are many oustanding procedures concerning the production of diffraction gratings with coherent light, including the grating for the moire interferometry method [5]. POST, PATORSKI and NING [6] have proposed recently a method for

producing 1200 *l*/mm crossed-line photoresist gratings of high diffraction efficiency using spatially and temporally incoherent light. The recorded interferograms are used as matrices to impress phase reflective gratings on a specimen under study.

The purpose of this paper is to analyse the recording of diffraction gratings by using two point sources of coherent light. The theory of the interference of two spherical wavefront beams is already well-known. The application of beams of this type to produce gratings for the moire interferometry method and subsequently to illuminate the specimen grating in the interferometer causes, however, some specific problems. On the one hand, the production of gratings using spherical wavefront beams is simple and economic. On the other hand, however, spherical wavefronts as well as finite distances between the sources and the recording plate might introduce deformation and asymmetry of the recorded fringe pattern. The theoretical cosiderations are verified by experiments.

2. Analysis

To analyze the fringe pattern due to two spherical wavefront beams, either the equation of family of hyperbolas [7] or nonparabolic approximation of a spherical wavefront can be used [8]. The second way of description is simpler and more exact. It gives the information about the values of the grating period as well as about the value of aberrations (deformations). For comparison, both the methods are presented.

2.1. Grating recording with an ideal arrangement

The interference produced by two point sources S_1 and S_2 is recorded on the plate P (Fig. 1). The wavefronts in this plane can be described as

$$V_j(x, y, z_0) = V_0 \exp(ikr_j), \quad j = 1, 2 \tag{1}$$

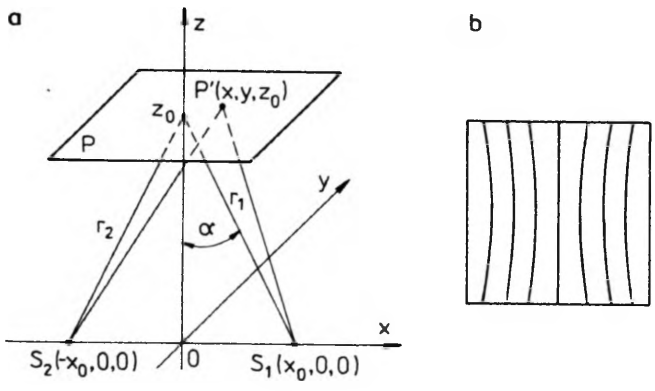

Fig. 1. Schematic diagram of recording a linear diffraction grating (**a**). P – recording plate, S_1 and S_2 – point sources, α – angle of illumination, r_1 and r_2 – distances between an arbitrary point P' of plane P and sources S_1 and S_2, respectively. The fringe pattern recorded on plate P(**b**)

where x and y are the coordinates, z_0 is the distance between the sources and the plate P, V_0 is a constant, $k = 2\pi/\lambda$, is the light wavelength, r_1 and r_2 stand for distances between an arbitrary point $P'(x, y, z_0)$ and the sources S_1 and S_2, respectively. Bright interference fringes appear when

$$k(r_1 - r_2) = n2\pi, \qquad n = 0, \pm 1, \pm 2, \ldots . \tag{2}$$

Assuming that the sources S_1 and S_2 are placed symmetrically with respect to the setup axis, that is, $x_1 = x_0$ and $x_2 = -x_0$, the distances r_1 and r_2 are equal, respectively, to

$$r_{1,2} = [(x \mp x_0)^2 + y^2 + z^2]^{1/2}. \tag{3}$$

Substituting the values of r_1 and r_2 to Eq. (2) we obtain the formula

$$\frac{x^2}{(n\lambda/2)^2\left[1 + \dfrac{z_0^2}{x_0^2 - (n\lambda/2)^2}\right]} - \frac{y^2}{x_0^2 + z_0^2 - (n\lambda/2)^2} = 1, \tag{4}$$

which describes a family of hyperbolas. The shape of each hyperbola depends on the parameters of illumination x_0, z_0, λ and the fringe number n. The n-th fringe satisfies the equation

$$x_n(y) = (n\lambda/2)\left\{\left[1 + \frac{y^2}{x_0^2 + z_0^2 - (n\lambda/2)^2}\right]\left[1 + \frac{z_0^2}{x_0^2 - (n\lambda/2)^2}\right]\right\}^{1/2}. \tag{5}$$

Let us define, using Eq. (5), the main grating parameters:

– the period d_0 in the centre of the grating (recording plane)

$$d_0 = x_1(0) = \lambda/2\left[1 + \frac{z_0^2}{x_0^2 - (\lambda/2)^2}\right]^{1/2}, \tag{6}$$

– the period d_s in the marginal region of the grating

$$d_s = x_n(y_{\max}) - x_{n-1}(y_{\max}), \tag{7}$$

where $x_n(y_{\max})$ and $x_{n-1}(y_{\max})$ are the respective coordinates of n-th and $(n-1)$-th fringes for the maximum value of y,

– the departure δ_s of the n-th fringe

$$\delta_s = |x_n(y_{\max}) - x_n(y = 0)|. \tag{8}$$

It appears that when the relative change of the grating period $\left|\dfrac{d_s - d_0}{d_0}\right|$ is about 10^{-3}, the value of δ_s/d_0 equals 0.1–0.2. It indicates that the parameter δ_s determines the quality of the grating produced by using two point sources. While designing the recording setup one should mostly pay attention to this parameter. Figure 2 shows the graph of δ_s as a function of distance z_0 when recording 600 and 1200 l/mm, 30×30 mm^2 grating with waves $\lambda = 0.6328$ μm. Note that by increasing the distance z_0 over 4–5 meters, no major improvements of the parameter δ_s are achieved. The

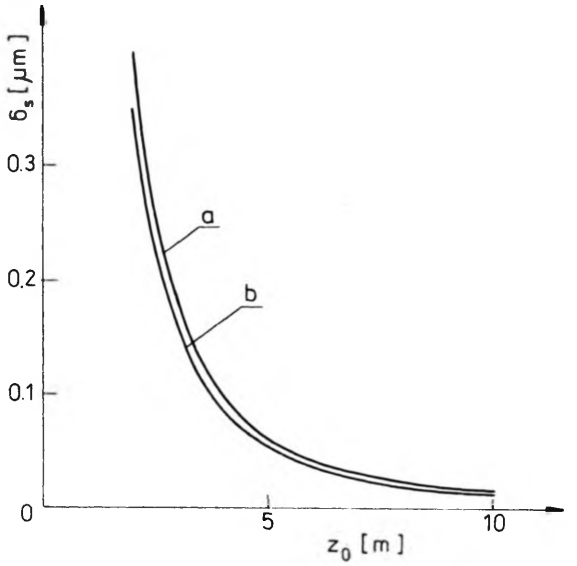

Fig. 2. Graph of changes of departure δ_s for a fringe of 30×30 mm^2 grating lying at its boundary against the distance z_0: **a** $-v = 600$ l/mm, **b** $-v = 1200$ l/mm, $\lambda = 0.6328$ μm

optimal value of z_0 is equal to about 3 meters for 600 l/mm grating and about 4 meters for 1200 l/mm grating. Further increse of z_0 slightly improves δ_s but at the same time it makes the experiment more difficult (for example, the nonstability of interference fringes caused by vibrations). Obviously, for all these calculations the following relation between distances x_0 and z_0 holds

$$x_0 = z_0 \tan\alpha. \tag{9}$$

In the second approach we use the formula describing the phase in arbitrary point $Q(x, y)$ in the plane $X0Y$ from point source $S(x_0, y_0, z_0)$, see Fig. 3, [8]

$$\varphi(x,y) = \frac{2\pi}{\lambda}\left[\frac{1}{2z_0}(x^2+y^2-2xx_0-2yy_0) - \frac{1}{8z_0^3}\left\{(x^2+y^2)^2 - 4x_0x(x^2+y^2)\right.\right.$$
$$-4y_0y(x^2+y^2)+2x_0^2(3x^2+y^2)+2y_0^2(3y^2+x^2)+8xyx_0y_0-4xx_0^3-4yy_0^3-4xx_0y_0^2$$
$$\left.\left.-4yx_0^2y_0\right\}\right]. \tag{10}$$

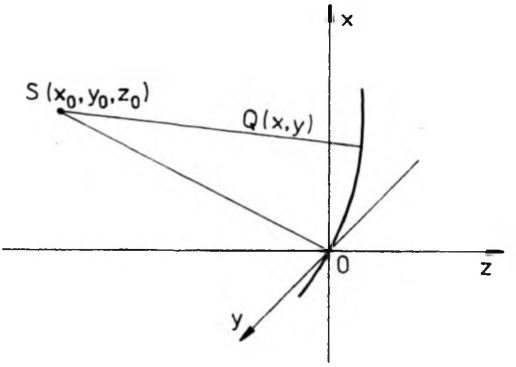

Fig. 3. Schematic diagram for calculating the phase distribution in the plane $X0Y$

The nonparabolic term in the Taylor series expansion of a function of a type $\sqrt{1-\varepsilon^2}$ is taken into account. The amplitude and phase distributions across the plane P (Fig. 1) from S_1 and S_2 are given by

$$V_{1,2}(x,y,z) = V_0 \exp\left\{ i\frac{2\pi}{\lambda}\left[\frac{1}{2z_0}(x^2+y^2 \mp 2xx_0) - \frac{1}{8z_0^3} \right.\right.$$
$$\left.\left. \times \{(x^2+y^2)^2 \mp 4x_0(x^2+y^2) + 2x_0^2(3x^2+y^2) \mp 4x_0^3 x\} \right]\right\} \tag{11}$$

where "−" and "+" relate to V_1 and V_2, respectively. The intensity distribution corresponds to the fringe equation of a recorded grating and is given by the formula

$$I(x,y,z_0) = 2V_0^2\left\{1+\cos\left[k\left\{\left(\frac{2x_0}{z_0}-\frac{x_0^3}{z_0^3}\right)x - \frac{x_0 x}{z_0^3}(x^2+y^2)\right\}\right]\right\}. \tag{12}$$

The grating period is

$$d = \frac{\lambda}{2\tan\alpha - \tan^3\alpha}, \tag{13}$$

and the grating lines deformation is

$$D = \frac{x_0}{z_0^3}x(x^2+y^2). \tag{14}$$

This deformation corresponds to an aberration function of coma. This method of description of the spherical wavefronts interference is simple and clear. It gives exact information about the grating period and the type and value of the grating lines deformation, which cannot be obtained by the method based on the equation of family of hyperbolas. To verify these calculations the table of the interference field frequency is presented. The frequencies are calculated for the same illumination angles α and light wavelength $\lambda = 0.6328$ μm.

I – two plane wavefronts interference,
II – two spherical wavefronts interference (Eq. (6)),
III – two spherical wavefronts interference (Eq. (13)).

Frequencies of the interference pattern obtained for the same illumination angles α and wavelength λ = 0. 6328 μm: I – plane, and II – spherical wavefronts interference

α			9.102°	10.943°	18.445°	22.314°
ν[l/mm]	I		500	600	1000	1200
	II	Eq. (6)	500	600	1000	1200
		Eq. (13)	499.9	599.7	995.5	1187.9
$\Delta\nu/\nu_{av}$ 100%			0.02	0.05	0.45	1.0

It is easy to notice that in the majority of cases the values of frequency $v = 1/d$ are almost equal. Only for $v = 1200\ l/\text{mm}$, when the value of illumination angle α is high, the relative error $\Delta v/v$ is equal to 1%. This testifies the correctness of the method.

2.2. Deformation of grating lines during the recording process

Let us observe now what happens to the fringes recorded when some errors occur in the recording system. In the experimental work the recorded pattern are used as reflective specimen gratings in the moire interferometer; the resulting interferograms will be presented.

2.2.1. Displacement Δ between the central interference fringe and the centre of the recording plate along the x direction

Figure 4 shows the sources of this error:

i) displacement Δ_x of the recording plate,

ii) displacement δ_x of one of the points sources,

both i) and ii) along the x direction. Figure 4c presents schematically the fringe pattern on the plate. It should be noticed that the shape of the fringes is still symmetrical with respect to the zeroth fringe, because of the constant distance z_0 between the sources and every point of plate P. From simple geometrical relations, it follows that the displacement Δ between the central interference fringe and the centre plate is equal to Δ_x and $\delta_x/2$, respectively. In order to describe the influence of displacement on the fringe pattern, we shall introduce a new coordinate system $X'\ Y'$ related to the plate P

$$x' = x - \Delta \rightarrow x = x' + \Delta, \tag{15a}$$

$$y' = y. \tag{15b}$$

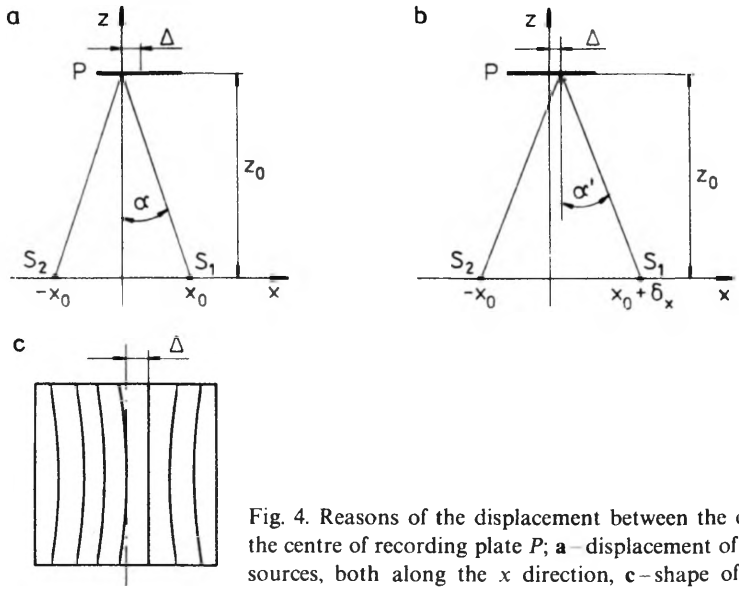

Fig. 4. Reasons of the displacement between the central interference fringe and the centre of recording plate P; **a** – displacement of the plate, **b** – one of the poin sources, both along the x direction, **c** – shape of the recorded fringes

The intensity distribution on the plate P (Eq. (12)), in these coordinates, can be described by

$$I(x', y', z_0) = 2V_0^2\left[1+\cos\left\{\frac{2\pi}{\lambda}\left[\left(\frac{2x_0}{z_0}-\frac{x_0^3}{z_0^3}\right)x' + \left(\frac{2x_0}{z_0}-\frac{x_0^3}{z_0^3}\right)\Delta - \frac{x_0}{z_0^3}x'(x'^2+y'^2) - \frac{x_0\Delta}{z_0^3}(3x'^2+y'^2)\right]\right\}\right] \tag{16}$$

where the terms with Δ^2 were omitted, as $\Delta \ll x_0$. The period of this interferogram is equal to that of the pattern recorded in an ideal arrangement (Eq. (13)). The fringes are deformed according to the comatic and astigmatic functions. The value of deformation decreases with the increasing distance z_0. Note that the astigmatic-type deformation appears solely due to the displacement Δ and disappears when $\Delta = 0$. This means that the grating described by Eq. (16), and used as the specimen grating in the moire interferometry setup, introduces into interferograms the aberrations of coma and astigmatism.

2.2.2. Displacement of the central interference fringe and asymmetry of the recorded pattern

Figure 5 shows the source of this error:

i) displacement δ_z of one of the point sources along the z direction,

ii) rotation of the recording plate around the axis parallel to the y axis.

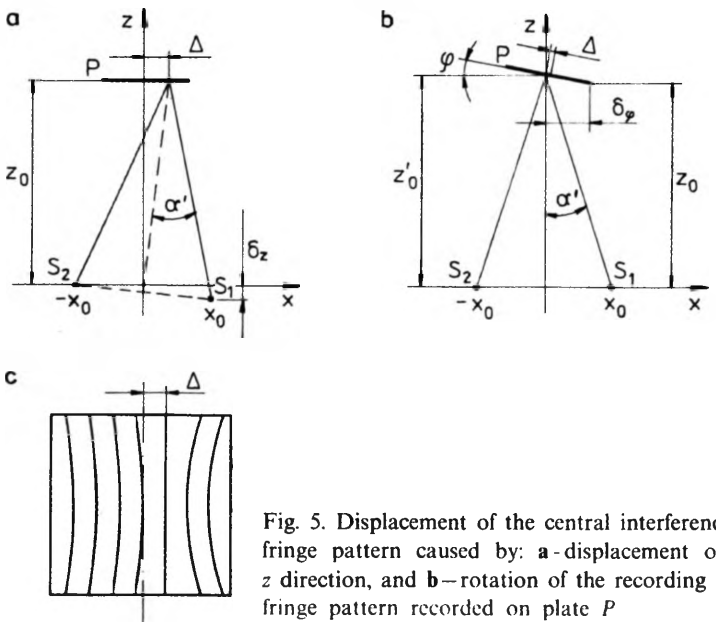

Fig. 5. Displacement of the central interference fringe and asymmetry of the fringe pattern caused by: **a** - displacement of one point source along the z direction, and **b** – rotation of the recording plate around the y axis, **c** – the fringe pattern recorded on plate P

The displacement Δ between the central fringe and the centre of the plate arising from these errors is respectively equal to:

$$\Delta_a = \frac{\delta_z}{2}\frac{z_0}{x_0}, \tag{17a}$$

$$\Delta_b = \frac{\varphi^2}{2}\delta_\varphi \tag{17b}$$

where φ is the angle of rotation, and δ_φ the displacement between the axis of rotation and the z axis. Since $\varphi \ll 1$, the displacement Δ_b equals nearly zero and can be omitted in further considerations. In both cases, the distance between the sources and an arbitrary point of the plate is no longer z_0, but

$$z_0' = z_0 + (x_0 + x - \Delta)\delta_z/2x_0. \tag{18}$$

For example, the difference between the distances z_0' and z_0 for 1200 l/mm grating, $z_0 = 4000$ mm, $\delta_z = 5$ mm and $\lambda = 0.6328$ μm is equal to 2.5 mm. This difference is not big, but, what is important, the changes of the distance z_0' introduce the asymmetry to the grating lines and next to the interferogram obtained in the moire interferometry. Using the coordinate system $X'Y'$ in the plate P(Eq. (15)) and introducing z_0' instead of z_0 into Eq. (12), we obtain

$$I(x', y', z_0) = 2V_0^2\left[1 + \cos\left\{2\pi/\lambda\left[\left(\frac{2x_0}{z_0} + \frac{x^3}{z_0^3}\right)x' + \left(\frac{2x_0}{z_0} - \frac{x_0^3}{z_0^3}\right)\Delta - \frac{x_0}{z_0'^3}x'(x'^2 + y'^2) - \frac{x_0\Delta}{z_0'^3}(3x'^2 + y'^2)\right]\right\}\right]. \tag{19}$$

The changes of grating period are the function of z_0'. The deformation of grating lines is described by the function of coma- and astigmatism-type. As the distance z_0' depends on the coordinate x (or x'), the grating period d changes along this direction bringing about the asymmetry of the recorded pattern and, subsequently, being the source of asymmetry of interferograms obtained in the moire interferometer.

2.2.3. Displacement of the centre of symmetry of the interference fringes along the y axis

Figure 6 shows the sources of this error

i) displacement δ_y of the point sources or the recording plate along the y axis,

ii) inclination of the plate by an angle γ.

The displacement Δ_y' between the centre of symmetry of the interference fringes and Δ_y'' of the centre of plate P along the y axis, due to the reasons mentioned above are:

$$\Delta_y' = \delta_y, \tag{20a}$$

$$\Delta_y'' = z_0\gamma, \tag{20b}$$

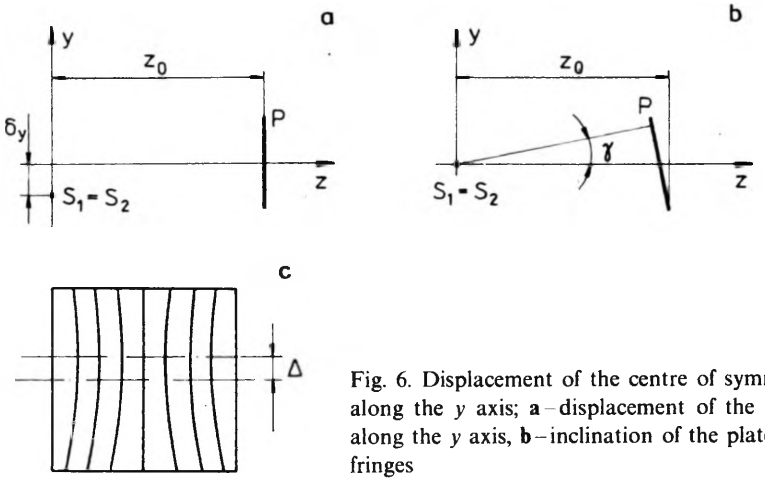

Fig. 6. Displacement of the centre of symmetry of the fringe pattern along the y axis; **a** – displacement of the point sources or the plate along the y axis, **b** – inclination of the plate, **c** – shape of the recorded fringes

respectively. If we compare Figure 6 to Figure 3, we can notice that, apart from the terms with x_0 (Eq. (10)), we should take into account the terms with y_0. In this case $y_0 = \Delta_y$. The intensity distribution on the plane P is given by

$$I(x, y, z_0) = 2V_0^2\left[1+\cos\left\{2\pi/\lambda\left[\left(\frac{2x_0}{z_0}-\frac{x_0^3}{z_0^3}\right)x-\frac{x_0}{z_0^3}x(x^2+y^2)\right.\right.\right.$$
$$\left.\left.\left.+\frac{2x_0\Delta_y}{z_0^3}xy\right]\right\}\right] \tag{21}$$

where terms with Δ_y^2/z_0^3 and Δ_y^3/z_0^3 are omitted, for $\Delta_y \ll z_0$. The period of this grating is constant and the deformation of grating lines is described by the comatic and astigmatic-type function.

2.2.4. Rotation of the fringe pattern about the z axis

This error is due to the following reasons:

i) sources are rotated about the z axis,

ii) the recording plate is rotated about the x axis.

After rotation of sources S_1 and S_2, their y coordinates are δ_y and $-\delta_y$ respectively. Introducing these values into Eq. (10), instead of y_0, we obtain the intensity distribution

$$I(x, y, z_0) = 2V_0^2\left[1+\cos\left\{\frac{2\pi}{\lambda}\left[\left(\frac{2x_0}{z_0}-\frac{x_0^3}{z_0^3}\right)x+\frac{2\delta_y}{z_0}y-\frac{x_0}{z_0^3}(x^2+y^2)\right]\right\}\right] \tag{22}$$

where the terms proportional to δ_y/z_0^3, δ_y^2/z_0^3, δ_y^3/z_0^3 were omitted, since $\delta_y \ll z_0$. In grating recorded in this way, the period and the deformation of its lines are similar to those in grating recorded under ideal conditions. However, the central interference

fringe is inclined to the edge of the plate by the angle β equal to

$$\beta = -\frac{2x_0 - x_0^3/z_0^3}{2\delta_y}. \tag{23}$$

Using such a grating in the moire interferometer, it is possible to obtain symmetrical interferograms. The inclination can be eliminated during the alignment of the setup.

2.2.5. Recording with two spherical wavefronts with different radii of curvature $R_1 \neq R_2$

This error occurs when the collimators are not exactly adjusted. Small value of defocus Δf results in a spherical wavefront of radius [9]

$$R = f^2/\Delta f - f \tag{24}$$

where f stands for the focal length. If the defocus values for the two beams are different, two spherical wavefronts with different radii of curvature interfere. The distances between the point sources of these wavefronts and the recording plate are

$$z_{0i} = R_i \cos\alpha, \qquad i = 1, 2 \tag{25}$$

where α is the illumination angle. Using Equation (10), the intensity distribution can be calculated as

$$\begin{aligned} I(x, y, z) = 2V_0^2 \Bigg[1 + \cos \Bigg\{ 2\pi/\lambda \Bigg[& (2\tan\alpha - \tan^3\alpha)\, x - (x^2 + y^2)\left(\frac{1}{2z_{02}} - \frac{1}{2z_{01}}\right) \\ & + \frac{1}{8}\left(\frac{1}{z_{02}^3} - \frac{1}{z_{01}^3}\right)(x^2 + y^2) - \frac{1}{2}\left(\frac{x_{02}}{z_{02}^3} - \frac{x_{01}}{z_{01}^3}\right) x(x^2 + y^2) \\ & + \frac{1}{4}\left(\frac{x_{02}^2}{z_{02}^3} - \frac{x_{01}^2}{z_{01}^3}\right)(3x^2 + y^2) \Bigg] \Bigg\} \Bigg] \end{aligned} \tag{26}$$

where $\tan\alpha = x_{01}/z_{01} = x_{02}/z_{02}$. The period of this pattern is constant and given by Eq. (13). The grating lines are deformed according to defocus, spherical aberration, coma and astigmatism functions.

3. Experimental work

The moire interferometer with the Lloyd mirror, shown in Fig. 7, has been used to verify the above presented principles. Gratings with the required deformations have been placed in the interferometer instead of the specimen grating SG. Their reflectivity is proportional to the intensity distribution recorded on the photographic plate and has the following form

$$R(x, y) = A_0 + \cos\left\{\frac{2\pi}{d}[x + u(x, y)]\right\} \tag{27}$$

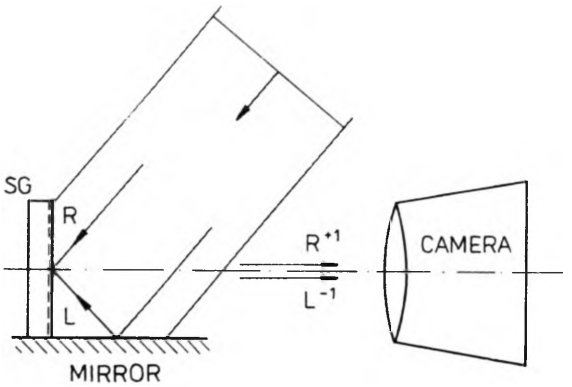

Fig. 7. Schematic representation of the moire interferometry setup used for checking the recorded gratings

where A_0 is a constant, d denotes the period of checked grating SG, and $u(x, y)$ is the function of the grating lines deformation. The grating SG is illuminated by plane wavefront beams R and L. Their incidence angles are slightly different from the first-order diffraction angle of the grating. The $+1$ diffraction order of the beam R and the -1 diffraction order of the beam L are respectively given by:

$$E^R_{+1}(x, y) = \exp\left[i\left(\frac{2\pi}{\lambda}\theta_{xi} + \frac{2}{d}u(x, y) + kw(x, y)\right)\right], \tag{28}$$

$$E^L_{-1}(x, y) = \exp\left[-i\left(\frac{2\pi}{\lambda}\theta_{x2} + \frac{2}{d}u(x, y) - kw(x, y)\right)\right] \tag{29}$$

where θ_{x1} and θ_{x2} are the angles between the normal of grating and beams R_{+1} and L_{-1}, respectively, λ is the light wavelength, and $w(x, y)$ is the out-of-plane displacement. The intensity distribution in the observation plane is

$$I(x, y) = A + \cos\left\{\frac{2\pi}{\lambda}[\theta_{xi} + \theta_{x2}]\, x + 2\frac{2\pi}{d}u(x, y)\right\} \tag{30}$$

where A is a constant. It means that the deformations of grating lines increase twofold in the interferogram. The recorded interferograms are presented to illustrate the above-mentioned cases. Figures 8**a** and 8**b** present two interferograms with different values of frequency and opposite signs of the carrier pattern of extension obtained for 600 *l*/mm grating recorded using two symmetrically placed sources. Interference fringes correspond to the aberration of coma visualized by the reference beam interferometer. The next interferogram (Fig. 8**c**) illustrates the deformation of 1200 *l*/mm grating recorded at the distance $z_0 = 1000$ mm, the recording plate being displaced along x direction. The fringe pattern is like the one obtained in the reference beam interferometer with the presence of the aberration of coma and astigmatism. The next interferogram (Fig. 8**d**) represents 1200 *l*/mm grating described by Eq. (26). It was produced using two spherical wavefront beams with different radii of curvature coming from two defocused collimator systems. Interference fringes have the form similar to a circle, and correspond to the defocus visualized by the reference beam interferometer.

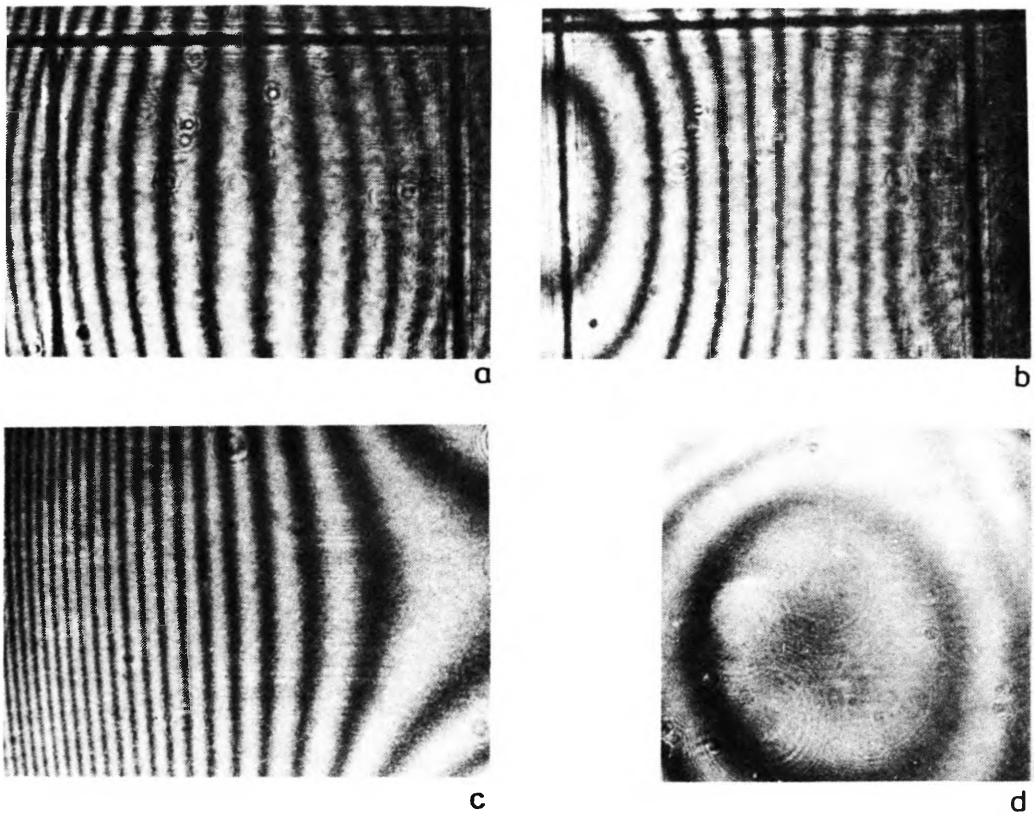

Fig. 8. Interferograms of checked gratings obtained under the following conditions: **a** and **b** – symmetrical recordings using two point sources of light (interferograms with different values of frequency and opposite signs of the carrier pattern of extension), **c** – one of the sources was shifted along the x direction, **d** – recording by using two non-plane wavefront beams

4. Conclusions

The analysis of the recording of the matrice gratings (molds) for the moire interferometry method using two spherical wavefront beams is presented. Two methods of description of the interference field are given. In the first one, the equation of hyperboles, and in the second the nonparabolic approximation of a sphere are used. The first method is better for design of the grating recording setup and for definition of parameters of the setup. The second method describes the interference of two spherical wavefronts, giving the value of the grating period and line deformations. When the setup is ideally aligned the interference fringes are deformed by comatic-type function. These deformations depend on the distance between light sources and the recording plate. They decrease when the distance increases. There is the optimal value of this distance and its further increase does not

improve straightness of the fringes but can introduce other difficulties resulting from vibrations, air turbulations, etc.

Inaccuracies in the recording setup alignment give typical deformations of the grating lines:

i) All displacements of the recording plate or the light sources along the directions of x and z axes introduce the astigmatic-type deformation: $A_x(3x^2+y^2)$.

ii) The forward or backward inclinations of the recording plate and the displacement of sources or the plate along y axis introduce the astigmatic-type deformation: $A_y xy$.

iii) The rotation of the plate or sources around z axis does not introduce additional deformation of the grating lines, but brings about an inclination of the grating lines against the edge of the plate. It can be eliminated in the moire interferometer by a suitable rotation of the specimen grating.

When the gratings are recorded using plane wavefront beams there may appear a defocus in the collimator system. In such a case two spherical wavefronts with different radii of curvature interfere. The grating recorded has a proper period but its lines are deformed by the following aberrations: defocus, spherical aberration, coma and astigmatism. As the deformations of grating lines double in the interferogram obtained in the moire interferometer, the quality of gratings must be as high as possible. The correctness of illumination arrangement can be checked putting, instead of a recording plate, the grating with either the same frequency or twice smaller than the desired one. The recorded gratings can be checked in the moire interferometry system. The deformations of grating lines are more or less complicated, and the obtained interferograms are charged with aberrations of many types. Nevertheless, if the interferograms corresponding to typical deformations of the grating lines are known, a dominant error made in the arrangement of the recording setup can be deduced.

Acknowledgement – I wish to thank Dr K. Patorski for his valuable remarks and suggestions concerning the final shape of this paper and for his continuous assistance during its preparation.

References

[1] Post D., Opt. Eng. **21** (1982), 458.
[2] McDonach A., McKelvie J., Mackenzie P., Walker C. A., Exp. Tech. **23** (1983), 20.
[3] Patorski K., Kujawińska M., Appl. Opt. **24** (1985), 3041.
[4] Patorski K., Appl. Opt. **25** (1986), 3146.
[5] Hutley M. C., *Diffraction Gratings*, Academic Press, New York 1982.
[6] Post D., Patorski K., Ning P., Appl. Opt. **26** (1987), 1100.
[7] Pawluczyk R., Mroz E., Opt. Acta **20** (1973), 379.
[8] Meier R. W., J. Opt. Soc. Am. **55** (1965), 987.
[9] Yokozeki S., Patorski K., Ohnishi K., Opt. Commun. **14** (1975), 401.

Received February 3, 1989
in revised form May 7, 1989

Производство решеток для муарной интерферометрии, употребляющей два пунктовых источника света

Представлены свойства решеток для муарной интерферометрии, регистрированных при употреблении двух точечных источников света. Результаты исследований показывают, что гиперболические линии этих решеток вводят аберрацию комы в интерферограмму, полученную в муарном интерферометре, а несимметрия в регистрирующей системе вводит астигматизм. Малые дефокусировки колиматоров, употребленных для регистрации решеток плоскими волнами, вводят все типы аберрации. Типичные интерферограммы могут помочь в устранении недостатков регистрирующей системы.